Submitted to The Astronomical Journal

H I Detection in two Dwarf S0 Galaxies in Nearby Groups: ESO384-016 and NGC 59

Sylvie F. Beaulieu

Département de Physique, de Génie Physique et d'Optique and Observatoire du mont Mégantic, Université Laval, Québec, Qc, G1K 7P4, Canada

sbeaulieu@phy.ulaval.ca

Kenneth C. Freeman

Research School of Astronomy and Astrophysics, Mount Stromlo Observatory, Weston Creek, ACT 2611, Australia

kcf@mso.anu.edu.au

Claude Carignan

Département de Physique and Observatoire du mont Mégantic, Université de Montréal, C.P. 6128, Succ. Centre-ville, Montréal, Qc, H3C 3J7, Canada

Claude.Carignan@umontreal.ca

Felix J. Lockman

National Radio Astronomy Observatory, P.O. Box 2, Green Bank, WV 24944, USA

jlockman@nrao.edu

and

Helmut Jerjen

Research School of Astronomy and Astrophysics, Mount Stromlo Observatory, Weston Creek, ACT 2611, Australia

jerjen@mso.anu.edu.au

ABSTRACT

An H I survey of 10 dE/dS0 galaxies in the nearby Sculptor and Centaurus A groups was made using the Australia Telescope Compact Array (ATCA). The observed galaxies have accurate distances derived by Jerjen et al (1998; 2000b) using the surface brightness fluctuation technique. Their absolute magnitudes are in the range $-9.5 > M_B > -15.3$. Only two of the ten galaxies were detected at our detection limit ($\sim 1.0 \times 10^6$ $\mathcal{M}_\odot$ for the Centaurus group and $\sim 5.3 \times 10^5$ $\mathcal{M}_\odot$ for the Sculptor group), the two dS0 galaxies ESO384-016 in the Centaurus A Group and NGC 59 in the Sculptor Group, with H I masses of $6.0 \pm 0.5 \times 10^6$ $\mathcal{M}_\odot$ and $1.4 \pm 0.1 \times 10^7$ $\mathcal{M}_\odot$ respectively. Those two detections were confirmed using the Green Bank Telescope. These small H I reservoirs could fuel future generations of low level star formation and could explain the bluer colors seen at the center of the detected galaxies. Similarly to what is seen with the Virgo dEs, the two objects with H I appear to be on the outskirt of the groups.

Subject headings: galaxies: dwarf — galaxies: individual (ESO384-016, NGC 59) — galaxies: evolution — galaxies: ISM

1. Introduction

The nature and origin of the fainter dwarf elliptical galaxies, and their relationship to the brighter ellipticals, remains poorly understood. Kormendy (1985) examined the structural scaling laws for the two classes of ellipticals (eg the correlations between absolute magnitude, core radius and effective surface brightness) and found a discontinuity between the scaling laws for the dwarf and brighter ellipticals. This discovery contributed significantly to the view that dwarf and giant ellipticals are formed by different processes. The issue remains controversial, however. Some authors (eg Jerjen & Binggeli 1997 ; Graham & Guzmán 2003) argue that the scaling law discontinuities are not fundamental but come from systematic changes of the surface brightness profiles with galaxy luminosity, such as the systematic changes of the index n of the empirical Sérsic law changes with luminosity.

Independent of the structural issues, there do appear to be three dynamical classes of ellipticals. The internal kinematics of ellipticals show some unambiguous changes with luminosity, with the breaks between classes located at $M_B \approx -17.5$ and $M_B \approx -19.5$ ($H_\circ = 75$ $\mathrm{km\,s^{-1}\,Mpc^{-1}}$). At $M_B \approx -17.5$, there is a marked transition in the dynamical properties between the intermediate luminosity ellipticals and the fainter dwarf ellipticals. The intermediate ellipticals ($-17.5 > M_B > -19.5$) appear to be dynamically isotropic and rotationally flattened (eg Davies et al 1983). Their "anisotropy" parameter $(V/\sigma)^*$, which measures the ratio of the observed value of (V/σ) to the value for an oblate isotropic

rotator with the observed ellipticity, is distributed around a mean of about 1 with small dispersion. For the fainter dwarf ellipticals, the mean values of $(V/\sigma)^*$ rapidly decrease as the magnitudes become fainter. Many of these fainter systems are found to have low or unmeasurable rotational velocities along their major axes (Bender & Nieto 1990; Bender et al 1991; Geha et al 2002, 2003; Simien & Prugniel 2002; Pedraz et al 2002; De Rijcke et al 2001). Figure 5 of van Zee, Skillman & Haynes (2004) shows the dynamical transitions nicely.

The dynamical transition between the intermediate luminosity ellipticals and the dwarfs is as dramatic and well-defined as the well-known transition at $M_B \approx -20$ between intermediate luminosity and giant ellipticals (Davies et al 1983). The brightest and faintest ellipticals both appear to be flattened by their anisotropic velocity distributions. These dynamical differences presumably reflect differences in the formation processes for the three classes of ellipticals.

While these formation processes are certainly not yet fully understood, we have at least a working picture for the formation of the two brighter dynamical classes of ellipticals. It seems likely that many of the brightest ellipticals form through mergers, which lead to their anisotropic velocity distribution (eg Naab & Burkert 2003), while the intermediate ellipticals are believed to form dissipatively and so end up rotationally flattened. At this time, the formation processes for the fainter dwarf ellipticals remain quite uncertain. They may have several formation routes. Bender & Nieto (1990) suggest that the anisotropic velocity distribution of the fainter dwarf ellipticals is generated by the anisotropic blowout of their interstellar medium by supernovae during their evolution and the subsequent dynamical readjustment. The fainter dwarf ellipticals presumably evolve from some kind of small star-forming systems, but these progenitor systems must have much lower angular momentum per unit mass than the rapidly rotating dwarf irregulars which we observe at the present time. Our lack of understanding of the fainter dwarf ellipticals makes it important to acquire as much information as possible about their dynamics and content.

The nearby Sculptor (Scl) and Centaurus A (Cen A) groups at mean distances of about 2.5 and 3.5 Mpc contain many dwarf irregular and dwarf elliptical galaxies. Côté et al (1997) made a study of the gas-rich dwarf irregular galaxies in these two groups, reaching down to $M_V = -8$, and others have supplemented this sample (eg Banks et al 1999). At the time, little was known about the gas-poor dE and dS0 population of these nearby groups. The fainter dE/dS0 galaxies usually have smooth low surface brightness light distributions. It is difficult to measure their radial velocities, and they cannot readily be distinguished from brighter galaxies at higher redshift on morphological grounds. Images are needed in which these objects are partly or wholly resolved into stars.

More recently, Jerjen et al. (1998, 2000a, 2000b) undertook an optical program to identify and study a complete sample of the gas-poor dE and dS0 galaxies in the Scl and Cen A groups. To confirm that their candidates were dwarf members of these groups, they used the Surface Brightness Fluctuation (SBF) technique developed by Tonry & Schneider (1988) to derive distances for their sample. Because these groups are so close, Jerjen et al. (1998, 2000a, 2000b) were able to reach dwarf galaxies four to five magnitudes fainter than those previously studied in the Virgo and Fornax clusters, and the groups Leo I, Dorado, NGC 1400, NGC 5044, and Antlia (eg Ferguson & Sandage 1990).

Jerjen et al (1998, 2000b) measured SBF distances for 5 faint dE/dSph galaxies in each of the Cen A and Scl groups. Their absolute magnitudes are in the range $\mathrm{M_B} = -9.5$ to -15.3. A few of these objects also have optical velocities to further confirm their group membership. Table 1 presents basic data for these 10 early-type dwarf galaxies in the Scl and Cen A groups.

We are interested in the origin of these dE/dSph galaxies: have they recently evolved from dIrr galaxies which have expelled their gas through star formation and stellar winds? It is already known that the fainter dE and dSph galaxies are not all totally gas-free; some contain detectable amounts of H I . For example, among the Local Group dwarf elliptical galaxies, NGC 147 has not been detected in H I but NGC 205 and NGC 185 ($M_B = -16.0, -14.7$) have detected H I masses of about 7×10^5 $\mathcal{M}_\odot$ and 1×10^5 $\mathcal{M}_\odot$ respectively (Young & Lo, 1996, 1997).

Some of the fainter dSph galaxies in the Local Group may also contain detectable H I . The transition dSph/dIrr galaxy Phoenix (Carignan, Demers & Côté 1991; St-Germain et al. 1999) has $\sim 10^6$ $\mathcal{M}_\odot$ of H I detected. Observations of the Sculptor dSph (Carignan et al. 1998; Bouchard, Carignan & Mashchenko 2003), at a distance of 80 kpc, showed 2×10^5 $\mathcal{M}_\odot$ of H I located in two clouds displaced from its optical center, suggesting expulsion from the galaxy or possibly residual gas from an earlier star-forming stage. It is not yet clear whether this residual gas is in any way associated with the extended star formation history of this dSph galaxy (eg Grebel 1998). Blitz & Robishaw (2000) suggested that many of the Local Group dSph and dSph/dIrr galaxies contain significant masses of H I , often displaced by a few kpc from the centers of the galaxies. Many of the dSph galaxies are projected on fairly dense fields of small high velocity clouds (Putman et al 2002), and it is difficult to tell whether the H I near these galaxies is just a foreground HVC or is really part of the galaxy. A recent study of H I in the Local Group dSph galaxies by Bouchard, Carignan and & Staveley-Smith (2005) finds that only two (Scl and Tucana) can be distinguished from high velocity clouds at a fairly high level of confidence.

Surveys of galaxy clusters (Virgo: Binggeli et al. 1985; Fornax: Ferguson 1989; Centaurus: Jerjen & Dressler 1997) have revealed large populations of dwarf ellipticals relative

to the numbers in groups and the field. The cluster environment is clearly conducive to the formation of dwarf ellipticals, presumably by the transformation of other kinds of galaxies via harassment, ram pressure stripping and blowout. Conselice et al (2003) have compiled a sample of H I observations of Virgo cluster dE galaxies. Of the 48 dE galaxies observed, 5 were convincingly detected, with H I masses $\sim$ a few $\times 10^7$ $\mathcal{M}_\odot$. These 5 are all near the periphery of the cluster. The authors argue that they are probably gas-rich systems recently accreted by the cluster, and are in the process of transformation by stripping.

The Local Group dSph galaxies studied by Bouchard et al (2005) are mostly fainter than $M_B = -12$. The Virgo dE sample compiled by Conselice et al (2003) are mostly brighter than $M_B = -14$. In the absolute magnitude gap between the Virgo and Local Group samples, the Jerjen et al surveys of the nearby Cen A and Scl groups provide a sample of 10 dE galaxies with $M_B = -9$ to -15 which we have observed at 21cm with the ATCA. Only two were detected in H I and observed with the Green Bank Telescope (GBT), along with one non-detection. These two detections (ESO384-016 in Cen A and NGC 59 in Scl) are the subject of this paper. Images of the eight non-detected galaxies and the two detected galaxies are shown in Figure 1 and Figure 2 respectively.

2. Observations and Reduction

The H I observations for our ten galaxies were made with the Australia Telescope Compact Array (ATCA) in the 750 m configuration. The total integration time per galaxy was $\sim$ 12 hours, and included 10 min on a primary calibrator, and then a sequence of 5 min on a secondary calibrator and 50 min on source. For the two detected galaxies, the observations were taken on 1998 April 11 for ESO384-016, and on 1998 July 28 for NGC 59. Details of the observations can be found in Table 2. The noise levels for the observations of the undetected galaxies are similar to those given in the last row of Table 2.

Data reduction was conducted using the Multichannel Image Reconstruction, Image Analysis and Display package (MIRIAD/ATNF) (Sault et al. 1995) for calibrating the data. The NRAO package AIPS was used to extract the moments maps i.e. the H I column density, velocity field and velocity dispersion.

Both our galaxies suffer from an elongated synthesised beam because the ATCA is an E-W array (for these observations). The N-S resolution of our beam is degraded by a factor of 1/sin(dec) relative to the E-W resolution. For our two galaxies, this corresponds to beam profiles of $167'' \times 61''$ for NGC 59, and $91'' \times 58''$ for ESO384-016, for our maps produced with natural weighting. Although it is customary to convolve the data with a circular beam, in

our case, this strategy would mean sacrificing a significant amount of resolution in the E-W direction. This could potentially lead to unnecessary loss of information for small sources like our dwarf galaxies.

The three most luminous dwarfs in our sample, including ESO384-016 and NGC 59, were subsequently observed in the 21cm line with the 100m Green Bank Telescope (GBT) of the NRAO at an angular resolution of 9 arcmins. The receiver system temperature at zenith was 18 K, but because these galaxies are quite far south (ESO 269-066 was observed at an elevation of 6 deg), emission from the atmosphere added between 5 and 20 K to the system temperatures. The spectra covered about 1000 km s^{-1} at a velocity resolution of 1.2 km s^{-1}. Each galaxy was observed for 5 to 10 minutes in frequency-switched mode; a low-order polynomial was fit to each spectrum to remove residual instrumental baseline.

3. H I Content and Distribution

The H I distributions of NGC 59 and ESO384-016 are shown in Figure 3 and Figure 4. From the comparison with the beam shown in the bottom left corner of the maps, it can be seen that both are barely resolved. Once detected with the ATCA, NGC 59 and ESO0384-016 were also observed with the GBT, along with ESO269-066 which was an ATCA non-detection. The GBT observations gave similar results: the GBT spectra are shown in Figure 5.

Table 3 summarizes the velocity (heliocentric) data and gives the H I masses. For NGC 59, the optical and H I observations give very similar systemic velocities $\sim$358 km s^{-1}. For ESO384-016, while the 2 H I velocities give a similar result of 504 km s^{-1}, the optical velocity is nearly 60 km s^{-1} higher. Optical observations of such low surface brightness systems are difficult, and the H I determinations are surely more accurate: the H I velocities are adopted.

From the GBT single dish profiles, total fluxes of 1.53 Jy km s^{-1} and 2.72 Jy km s^{-1} and line widths (FWHM) of 33.7 $\pm$2.3 km s^{-1} and 50.6 $\pm$2.1 km s^{-1} were measured for ESO384-0166 and NGC 59, respectively. A mean of the ATCA and the GBT fluxes gives H I masses of $6.0 \pm 0.5 \times 10^6$ $\mathcal{M}_\odot$ for ESO384-016 and $1.4 \pm 0.1 \times 10^7$ $\mathcal{M}_\odot$ for NGC 59. From the noise in the ATCA maps and assuming a line width of 40 km s^{-1} ($\approx$ mean for our two detections), we can put an upper (3-σ) limit of $\sim 5.3 \times 10^5$ $\mathcal{M}_\odot$ on the H I content of the non-detected objects in Sculptor ($\Delta \sim 2.5$ Mpc) and $\sim 1.0 \times 10^6$ $\mathcal{M}_\odot$ in the Centaurus group ($\Delta \sim 3.5$ Mpc).

4. Discussion and Conclusion

As we have seen, the two galaxies that were detected are dS0s while all the other galaxies in the sample are dEs. Looking at their optical properties in Jerjen et al. (2000a), it can be seen that those two types are quite different, e.g. their surface brightness profiles (see Fig. 3 of Jerjen et al. 2000a). While the profiles for dEs tend to flatten in the very inner parts, those of dS0s stay linear all the way to the center and sometimes even exhibit what looks like a bulge component. Their best-fitting Sérsic profiles give Sérsic n values for our 2 dS0s of n $\sim$ 0.7 (n = 0.25 for a de Vaucouleurs profile) , while for the dEs $1.2 < n < 1.7$. This change of slope in the gradient of the radial light distribution is what was used by Sandage and Binggeli (1984) to define the dS0 class. Later, Binggeli & Cameron (1991) gave five main criteria to classify a system as dS0 instead of dE: (*i*) unusual King parameters; (*ii*) high flattening; (*iii*) presence of a lens; (*iv*) asymmetry (change of ellipticity, presence of a bar, isophotal twists, boxiness); and (*v*) central irregularity (clumpiness).

The present study suggests another difference: the high H I content. While for the few nearby dEs where H I is detected, such as NGC 185 and NGC 205 (Young & Lo 1997), the M_{HI}/L_B is very small (0.004 and 0.003, respectively), the M_{HI}/L_B of ESO384-016 and NGC 59 are much larger at 0.21 and 0.07, respectively. Those M_{HI}/L_B are similar to what is seen in dSph/dIrr galaxies such as Phoenix ($M_{HI}/L_B \sim 0.21$; St-Germain et al. 1999). In terms of their H I content, they are closer to dIrrs such as GR 8 (Carignan et al. 1990) and Sextans A (Skillman et al. 1988) which have $M_{HI}/L_B \sim 1.0$ than to dEs. In fact, their M_{HI}/L_B is similar to the H I content seen in a normal spiral like the MW ($M_{HI}/L_B \sim 0.18$).

Looking at the total H I maps, not much can be said about NGC 59 since it is not really resolved. However, the resolution is slightly better for ESO384-016. Fig. 4 indicates that the contours are somewhat compressed on the west side with an elongated component extending to the east. This is what we might expect if this system is falling toward the center of the Centaurus Group and was in interaction with its intergalactic medium (IGM). ESO384-016 lies on the east side of the group, so the orientation of these features is in the expected direction. This is reminescent of what is seen in Holmberg II (Bureau & Carignan 2002) which is thought to be falling toward the center of the M81 Group.

The color-magnitude diagram for the galaxies in our sample is shown in Figure 6. The two detected dS0 are amongst the brightest, with $M_B < -13$. The galaxies in the two groups are well separated in color, with the Sculptor systems having $(B-R)^0_T \leq 1.1$ and the Centaurus galaxies $(B-R)^0_T \geq 1.1$. It is more interesting to look at the radial color profiles of the galaxies in the sample (Fig. 4 of Jerjen et al. 2000a). The two detected galaxies are those with the largest color gradient, with $(B-R)^0_T$ varying from 0.60-0.85 in the center to ~ 1.5 in the outer parts. While the colors in the outer parts are typical of E-S0 galaxies, the

colors in the center are more like what is seen in late-type spiral and irregular galaxies. This may indicate that recent star formation has taken place in the center of those two galaxies using some of the gas from the detected H I reservoirs.

The only other sample with which our results could be compared to is the Conselice et al. (2003) Virgo dE sample. The distribution of the two samples as a function of absolute magnitude is shown in Figure 7. It can be seen that while our objects are mostly fainter than $M_B \sim -14$ (9/10), most of the Virgo galaxies are around $M_B \sim -16$. However, our M_{HI}/L_B are only slightly smaller than their mean M_{HI}/L_B of 0.36 ± 0.16 while their mean H I mass is a factor of ~ 10 larger at $<\mathcal{M}_{HI}> = 2.8 \times 10^8$ $\mathcal{M}_\odot$ (Figures 8 & 9). Comparing the location of our two detected galaxies (Figures 10 & 11) to the detected systems in Virgo (Fig. 5 of Conselice et al. 2003) we see that, as in Virgo, our H I -detected systems are found near the periphery of the groups.

The main results of this paper are:

- Of the 10 dE/dSO of the Sculptor and Centaurus groups observed with the ATCA, only the two dS0s ESO384-016 and NGC 59 were detected at 21cm with our detection limit of $\sim 1.0 \times 10^6$ $\mathcal{M}_\odot$ for the Centaurus group and $\sim 5.3 \times 10^5$ $\mathcal{M}_\odot$ for the Sculptor group. These two detections were subsequently confirmed with GBT observations.
- The two detected systems also happen to be among the most luminous early-type dwarf galaxies in the two groups with M_B = –15.3 & –13.2
- We find H I masses of $1.4 \pm 0.1 \times 10^7$ $\mathcal{M}_\odot$ for NGC 59 and $6.0 \pm 0.5 \times 10^6$ $\mathcal{M}_\odot$ for ESO384-016.
- The H I properties (mass, M_{HI}/L_B) of NGC 59 and ESO384-016 are much closer to those of dIrrs or normal spirals than of dEs.
- Features in the H I distribution of ESO384-016 suggest that it may be experiencing ram pressure stripping from the Centaurus Group IGM while falling toward the centre of the group.
- The $(B-R)^0_T$ colors of the two detected galaxies suggest that recent star formation has taken place from the reservoir of detected gas.
- Our two detected galaxies appear to have similar M_{HI}/L_B than the ones of the detected dwarfs in the Virgo cluster and, as in Virgo, they are located on the outskirt of the groups.

As in the Local Group, we expect that more sensitive observations would succeed in detecting HI reservoirs in or close to dEs (dS0s, dSph, dSph/dIrr) in nearby groups. We know from population studies that, in some of those systems, H I is needed to explain the presence of the observed young or intermediate age populations (Grebel et al 2003). The two systems presented here were detected after only 5-10 minutes observations with the GBT. With the much improved radio receivers ($T_{sys} \leq 20$ K), it is surely worthwhile to do much deeper observations of those galaxies. The knowledge of their ISM content and kinematics are essential ingredients if we want to understand the evolution of dwarf systems and pin down the progenitors of the present-day dEs.

SFB wishes to acknowledge financial support from the Institute of Astronomy, Cambridge (through grants from PPARC), for financing all the ATCA observing runs of this project. SFB is also grateful for the assistance from Tasso Tzioumis for observing one galaxy during a period of flooded roads, Kate Brooks, Haida Liang, Stéphanie Côté and Bob Sault for their help and discussion. CC acknowledges support from NSERC (Canada). Based on photographic data obtained using the UK Schmidt Telescope. The UK Schmidt Telescope was operated by the Royal Observatory Edinburgh, with funding from the UK Science and Engineering Research Council, until 1988 June, and thereafter by the Anglo-Australian Observatory. Original plate material is copyright (c) the Royal Observatory Edinburgh and the Anglo-Australian Observatory. The plates were processed into the present compressed digital form with their permission. The Digitized Sky Survey was produced at the Space Telescope Science Institute under US Government grant NAG W-2166. The National Radio Astronomy Observatory is operated by Associated Universities, Inc., under a cooperative agreement with the National Science Foundation.

REFERENCES

Banks, G.D., Disney, M.J., Knezek, P.M. et al 1999, ApJ, 524, 612

Bender, R., & Nieto, J.-L. 1990, A&A, 239, 97

Bender, R., Paquet, A., & Nieto, J.-L. 1991, A&A, 246, 349

Binggeli, B., & Cameron, M. 1991, A&A, 252, 27

Binggeli, B., Sandage, A., & Tammann, G.A. 1985, AJ, 90, 1681

Blitz, L., & Robishaw, T. 2000, ApJ, 541, 675

Bouchard, A., Carignan, C., & Mashchenko, S. 2003, AJ, 126, 1295

Bouchard, A., Carignan, C., & Staveley-Smith, L. 2005, in preparation

Bouchard, A., Jerjen, H., Da Costa, G.S., & Ott, J. 2005, AJ, accepted

Bureau, M. & Carignan, C. 2002, AJ, 123, 1316

Carignan, C., Beaulieu, S., Côté, S., Demers, S. & Mateo, M. 1998, AJ, 116, 1690

Carignan, C., Beaulieu, S., & Freeman, K. C. 1990, AJ, 99, 178

Carignan, C., Demers, S. & Côté, S. 1991, ApJ, 381, L13

Conselice, C. J., O'Neil, K., Gallagher, J. S., & Wyse, R. F. G. 2003, ApJ, 591, 167

Côté, S., Freeman, K. C., Carignan, C. & Quinn, P. J. 1997, AJ, 114, 1313

Davies, R.L., Efstahiou, G, Fall, S.M., Illingworth, G. & Schechter, P.L. 1983, ApJ, 266, 41

De Rijcke, S., Dejonghe, H., Zeilinger, W. W., & Hau, G.K.T. 2001, ApJ, 559, L21

Ferguson, H.C. 1989, AJ, 98, 367

Ferguson, H.C., & Sandage, A. 1990, AJ, 100, 1

Geha, M., Guhathakurta, P., & van der Marel, R. P. 2002, AJ, 124, 3073

Geha, M., Guhathakurta, P., & van der Marel, R. P. 2003, AJ, 126, 1794

Gooch, R.E. 1997, PASA, 14, 106

Graham, A.W., & Guzmán, R. 2003, AJ, 125, 2936

Grebel, E. K. 1998, in Highlights of Astronomy, Joint Discussion 14 of the XXIIIrd General Assembly of the IAU, Edited by Johannes Andersen, Kluwer Academic Press, Vol. 11, p. 125

Grebel, E. K., Gallagher, J. S. & Harbeck, D. 2003, AJ, 125, 1926

Jerjen, H., Binggeli, B. 1997, in ASP Conf. Ser. 116, The Second Stromlo Symposium: The Nature of Elliptical Galaxies, eds M. Arnaboldi, G.S. Da Costa & P. Saha (San Francisco: ASP), 239

Jerjen, H. & Dressler, A. 1997, A&AS, 124, 1

Jerjen, H., Freeman, K.C. & Binggeli, B. 1998, AJ, 116, 2873

Jerjen, H., Binggeli, B., & Freeman, K.C. 2000a, AJ, 119, 593

Jerjen, H., Freeman, K.C. & Binggeli, B. 2000b, AJ, 119, 166

Kormendy, J. 1985, ApJ, 295, 73

Naab, T. & Burkert, A. 2003, ApJ. 597, 893

Pedraz, S., Gorgas, J., Cardiel, N., Sánchez-Blázquez, P. & Guzmán, R. 2002, MNRAS, 332, L59

Putman, M. E., de Heij, V., Staveley-Smith, L., Braun, R., Freeman, K. C., et al. 2002, AJ, 123, 873

Sandage, A., & Binggeli, B. 1984, AJ, 89, 919

Sault, R.J., Teuben, P.J., & Wright, M.C.H. 1995, Astronomical Data Analysis Software and Systems IV, ASP Conference Series, Volume 77, eds. R.A. Shaw, H.E. Payne, & J.J.E. Hayes, 4, 433

Simien, F.& Prugniel, Ph. 2002, A&A, 384, 371

Skillman, E. D., Terlevich, R., Teuben, P. J., & van Woerden, H. 1988, A&A, 198, 33

St-Germain, J., Carignan, C., Côté, S., Oosterloo, T. 1999, AJ, 118, 1235

Tonry, J. & Schneider, D.P. 1988, AJ, 96, 807

van Zee, L., Skillman, E. D., & Haynes, M. P. 2004, AJ, 128, 121

Young, L. M., & Lo, K. Y. 1996, ApJ, 464, L59

Young, L. M., & Lo, K. Y. 1997, ApJ, 476, 127

Table 1. Parameters of the galaxies in the sample (Jerjen et al. 1998, 2000b)

Galaxy (1)	Type (2)	R.A. (J2000) (3)	Decl. (J2000) (4)	M_B^0 (mag) (5)	$(B-R)_T^0$ (mag) (6)	D (Mpc) (7)	V_{opt}[a] ($\mathrm{km\,s^{-1}}$) (8)	V_{HI}[ab] ($\mathrm{km\,s^{-1}}$) (9)
Centaurus A Group								
ESO219-010	dE,N	12 56 09.6	−50 08 38	-12.78	1.32	4.8(0.4)	···	···
ESO269-066	dE	13 13 09.5	−44 52 56	-13.66	1.48	4.0(0.5)	784(32)	···
AM1339-445	dE	13 42 05.8	−45 12 21	-12.09	1.38	3.7(0.5)	···	···
AM1343-452	dE	13 46 17.8	−45 41 05	-11.08	1.35	4.0(0.7)	···	···
ESO384-016	dS0	13 57 01.2	−35 19 59	-13.21	1.09	4.2(0.1)	561(32)	···
Sculptor Group								
NGC59	dS0	00 15 25.1	−21 26 38	−15.30	1.07	4.4(0.2)	362(10)	367 (357 in Hα)
SC22[c]	dE	00 23 51.7	−24 42 18	−9.50	0.79	2.7(0.2)	···	···
ESO294-010	dS0/Im	00 26 33.4	−41 51 19	−10.67	1.17	1.7 (0.1)	117(5)	···
ESO540-030	dE/Im	00 49 21.1	−18 04 34	−11.22	0.83	3.2 (0.1)	···	···
ESO540-032	dE/Im	00 50 24.5	−19 54 23	−10.39	1.08	2.2 (0.1)	···	···

[a]Heliocentric velocities

[b]Parkes HI single dish velocity from Côté et al. 1997

[c]a.k.a. Scl-dE1 (Jerjen et al. 1998)

Table 2. H I Observations for ESO384-016 and NGC 59

	ESO384-016	NGC 59
Array Configuration	750A	750E
Receiver (cm)	20	20
Integration Time (hr)	11.68	11.47
Transition (MHz)	H I 1420	H I 1420
Channel Bandwidth (kHz)	15.6	15.6
Velocity Increment ($\mathrm{km\,s^{-1}}$)	3.3	3.3
Number channel per baseline	512	512
Correlator Configuration	FULL	FULL
Primary Calibrator	PKS1934-638	PKS1934-638
Secondary Calibrator	PKS1320-446	PKS0023-263
Bandwidth (MHz)	8	8
Cell size (arcsec)	20	20
RMS noise (mJy/beam)	3.0	2.6
3σ/channel ($\mathrm{cm^{-2}}$)	7×10^{18}	3×10^{18}

Table 3. H I results for ESO384-016 and NGC 59

	Systemic V_{hel} ($\mathrm{km\,s^{-1}}$)			M_{HI} ($M_{\odot}$)		M_{HI}/L_B
	Optical	ATCA	GBT	ATCA	GBT	
ESO384-016	561	504	504	$5.6 \pm 0.3 \times 10^6$	$6.5 \pm 0.1 \times 10^6$	0.21
NGC 59	362	359	357	$1.5 \pm 0.3 \times 10^7$	$1.3 \pm 0.1 \times 10^7$	0.07

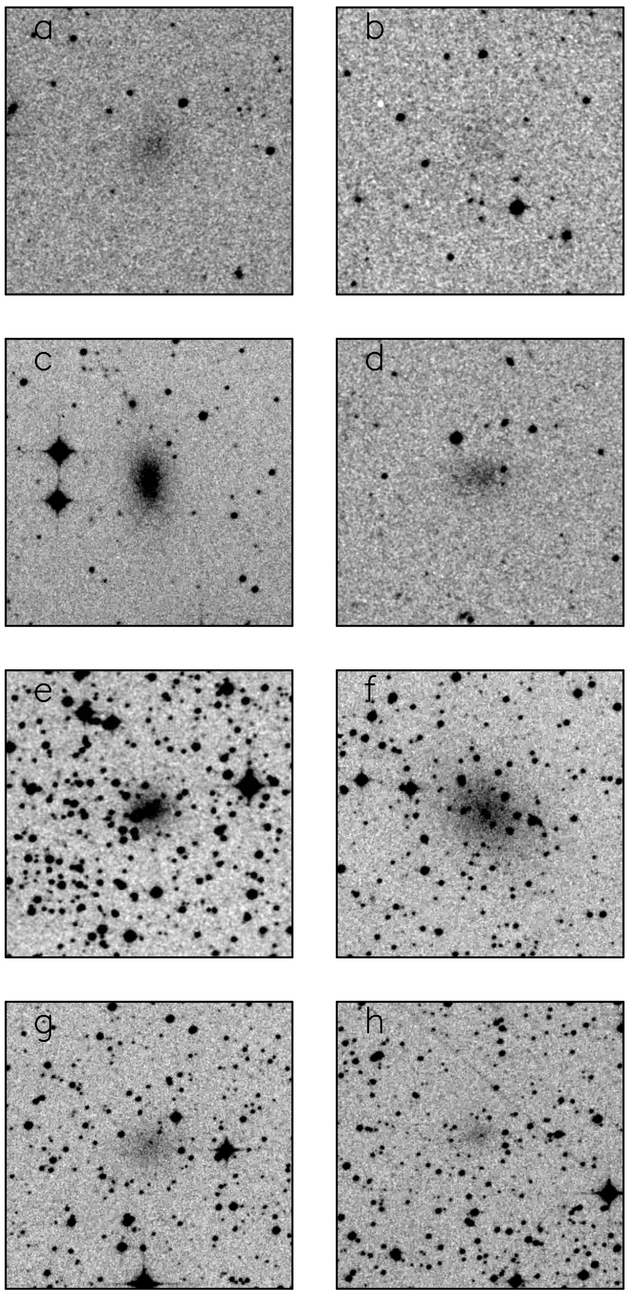

Fig. 1.— STScI DSS optical images of the 8 non-detections. The galaxies are: (a) ESO540-032, (b) SC22, (c) ESO294-010, (d) ESO540-030, (e) ESO219-010, (f) ESO269-066, (g) AM1339-445, and (h) AM1343-452. East is left and North is up. The FOV is $5' \times 5'$.

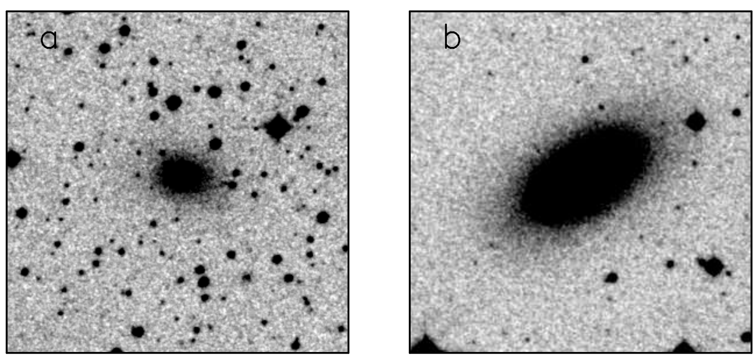

Fig. 2.— STScI DSS optical images of the 2 detections. The galaxies are: (a) ESO384-016, and (b) NGC 59. East is left and North is up. The FOV is $5' \times 5'$.

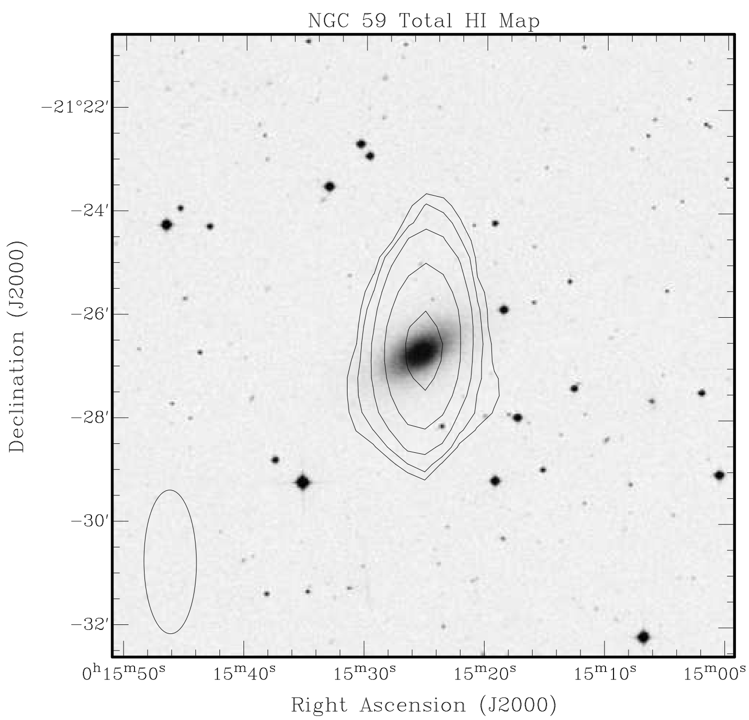

Fig. 3.— Total H I map of NGC 59 superposed on the STScI DSS optical image using the displaying package KARMA (Gooch 1997). The contours are $0.8, 1.6, 3.2, 6.4$ and 12.8×10^{19} cm^{-2}.

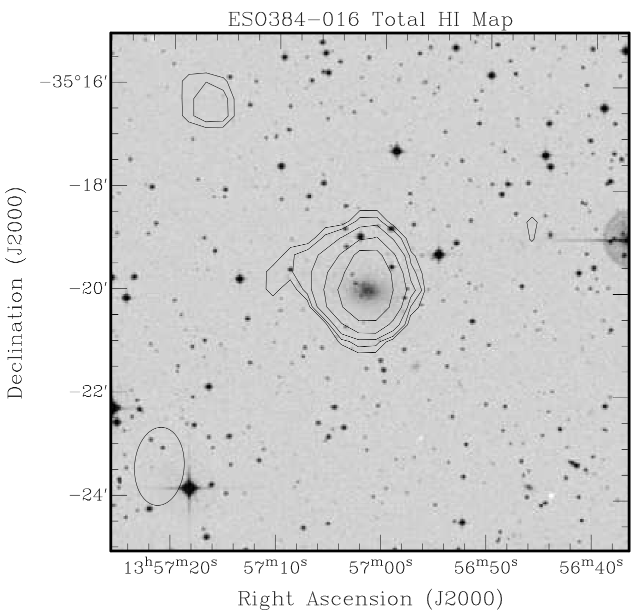

Fig. 4.— Total H I map of ESO384-016 superposed on the STScI DSS optical image using the displaying package KARMA (Gooch 1997). The contours are $0.5, 1.0, 2.0, 4.0,$ and 8.0×10^{19} cm^{-2}.

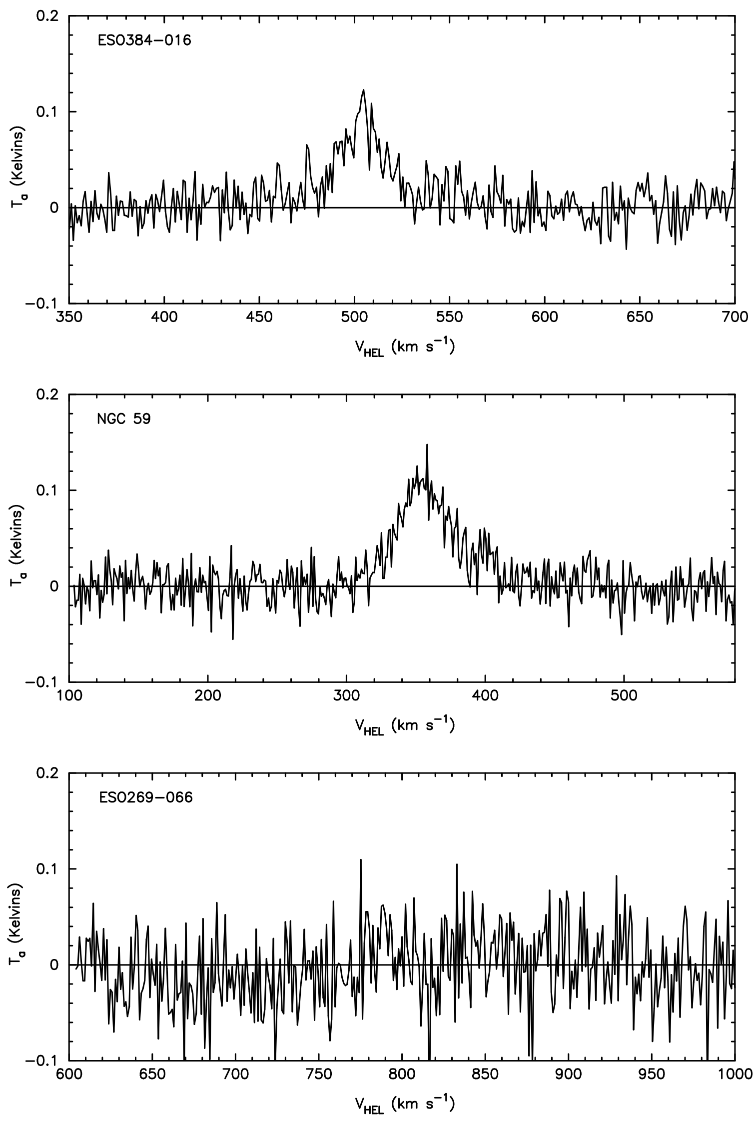

Fig. 5.— Single dish spectra from the GBT.

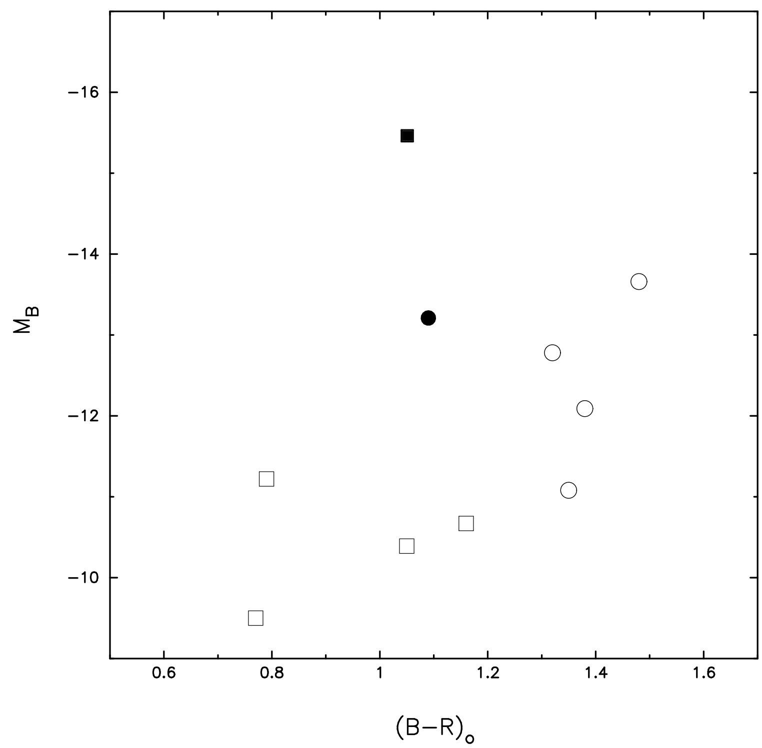

Fig. 6.— Color–Magnitude diagram for our sample. Squares are for Sculptor objects, circles for Centaurus and filled symbols are the detected dS0 galaxies.

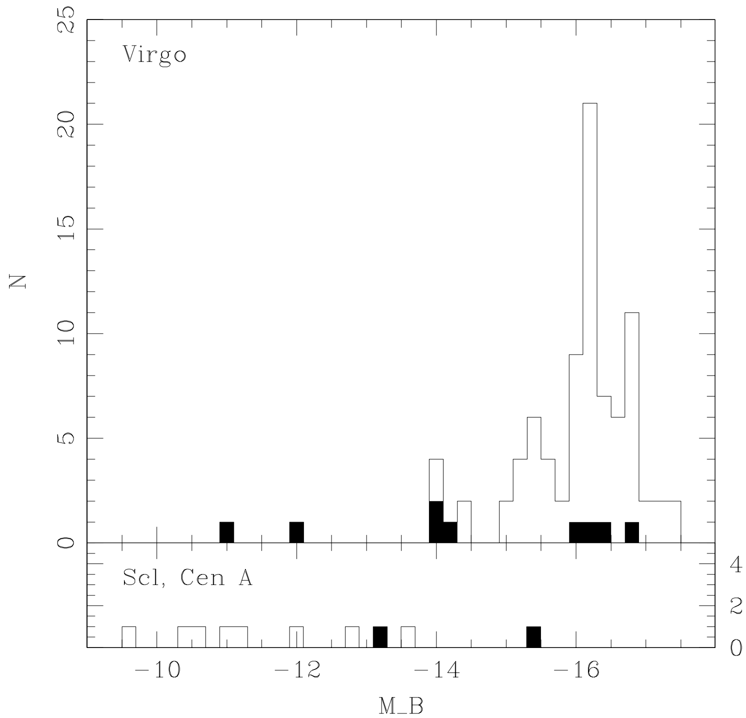

Fig. 7.— Distribution of the H I detected dwarfs in the Virgo sample of Conselice et al (2003) and in our Scl/Cen A sample, as a function of absolute magnitude.

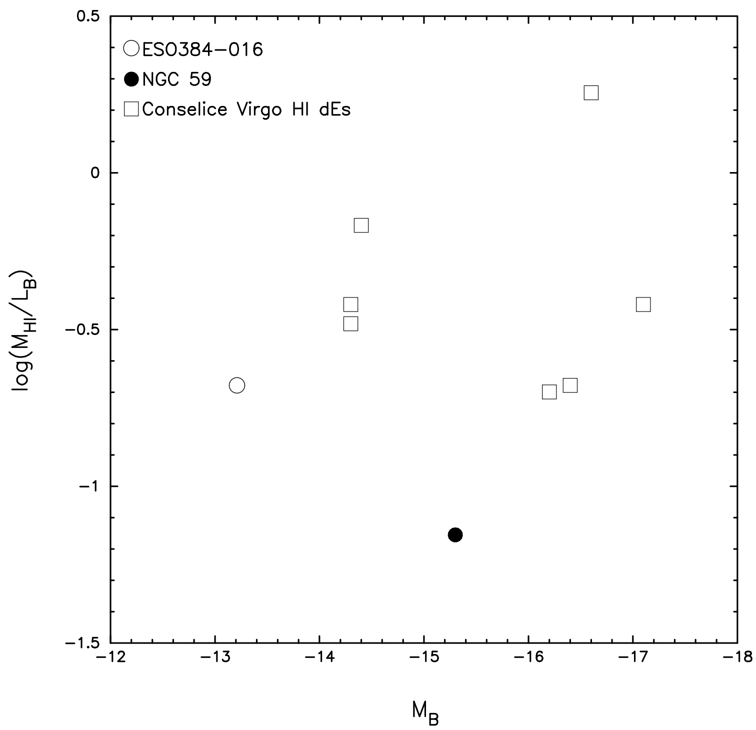

Fig. 8.— Absolute magnitude (M_B) vs. M_{HI}/L_B diagram for Virgo H I detected dE galaxies (Conselice et al 2003) and the H I detected dwarf galaxies in this study.

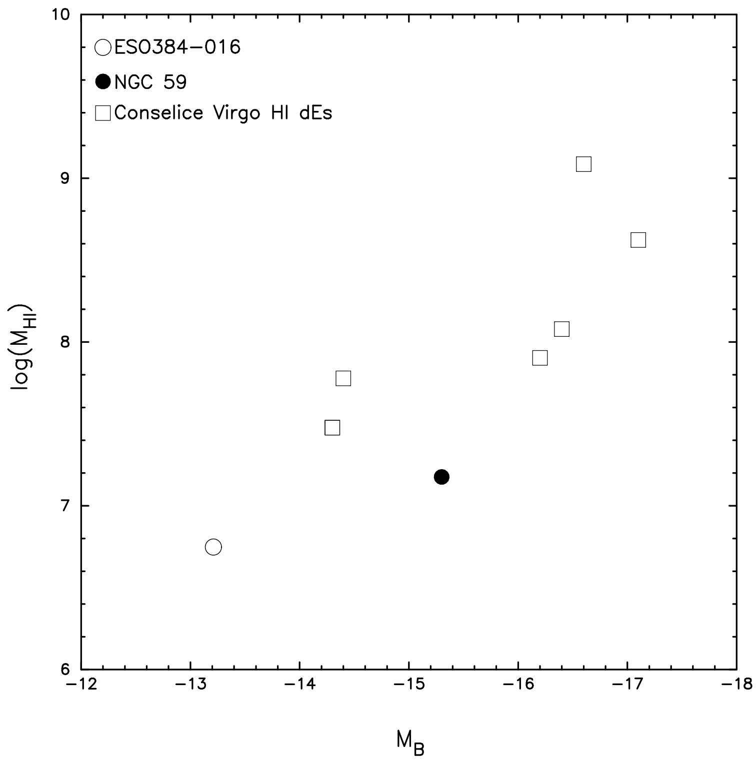

Fig. 9.— Absolute magnitude (M_B) vs. $\mathcal{M}_{HI}$ diagram for Virgo H I detected dE galaxies (Conselice et al 2003) and the H I detected dwarf galaxies in this study.

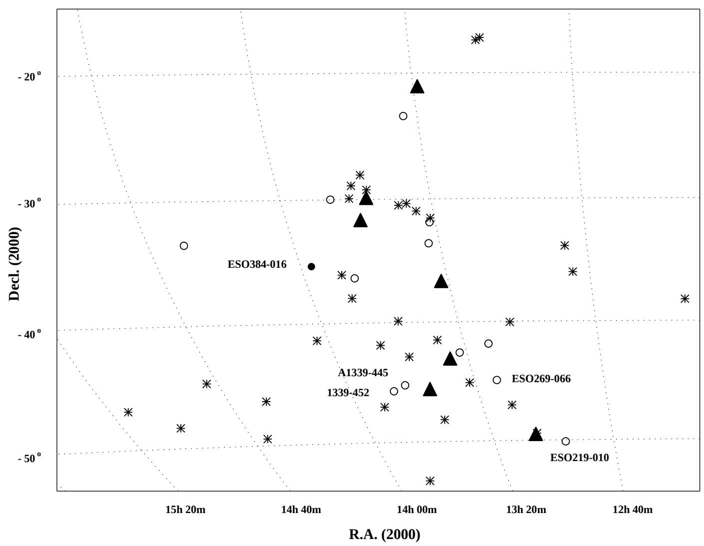

Fig. 10.— Distribution in R.A. (J2000.0) and Decl. (J2000.0) of the Cen A group. Filled triangles: major group members, stars: late-type dwarf galaxies (Côté et al 1997, Jerjen et al 2000b), unlabelled circles: early-type galaxies (Jerjen et al 2000a), labelled circles: early-type galaxies observed in this study, labelled filled circle: early-type galaxy ESO384-016 observed in this study with HI detected.

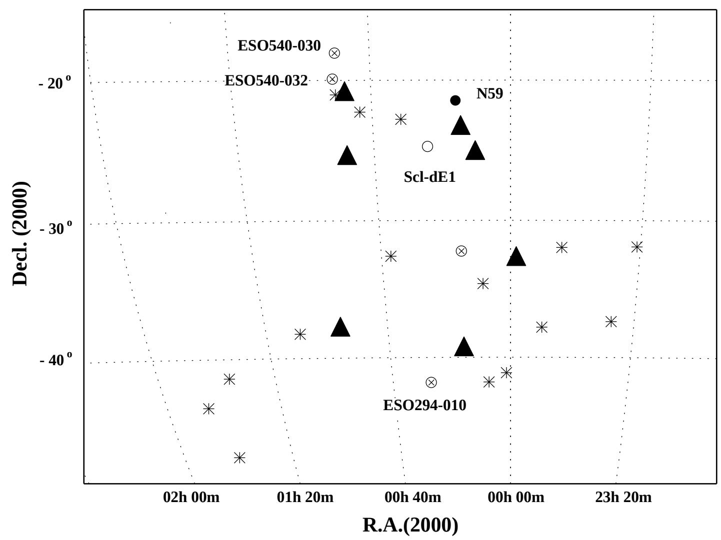

Fig. 11.— Distribution in R.A. (J2000.0) and Decl. (J2000.0) of the Scl group. Filled triangles: major group members, stars: late-type dwarf galaxies (Côté et al 1997), circle: early-type galaxy Scl-dE1 (SC22) observed in this study, but not detected in HI, labelled filled circle: early-type galaxy NGC59 observed in this study with HI detected, labelled crossed circle: early-type galaxies observed in this study with no HI detected at our detection limit of $\mathcal{M}_{HI} = \approx 10^7\, \mathcal{M}_\odot$, but HI detected at the $\mathcal{M}_{HI} = \sim 10^{(5-6)}\, \mathcal{M}_\odot$ level (Bouchard, Jerjen, Da Costa & Ott, 2005), unlabelled crossed circle: early-type galaxies ESO410-005, not observed in our study but detected in HI by Bouchard, Jerjen, Da Costa & Ott (2005).